The coefficients of this linear combination $[x(i)]$ put the intensities of the peaks in phase i on the absolute scale. $I_{max}(i)$, the intensity calculated on the absolute scale for the strongest (100%) diffraction peak of phase i, gives the intensity diffracted by one unit cell (structure factors are calculated for the atoms of one unit cell). Then $x(i)/I_{max}(i)$ is the number of unit cells of phase i in the analysed volume. Consequently, the volume extended by phase i in the analysed volume is $V(i)x(i)/I_{max}(i)$, where $V(i)$ is the volume of the unit cell of phase i. The volume fraction of phase f_i is then given by

$$f_i = \frac{V(i)x(i)}{I_{max}(i)} \Big/ \sum_i \frac{V(i)x(i)}{I_{max}(i)}. \qquad (2.4.21)$$

In addition to volume fractions of phases and their fibre-textured components, the same method can determine the variation (contraction, dilation, distortions) of the unit cell, provided experimental parameters specific to electron diffraction (*e.g.* the camera length and pattern distortion) are properly calibrated. The reliability of the camera-length calibration (systematic error) is usually around 2% (Williams & Carter, 2009); in the best cases accuracy of better than 0.3% has been reported (Lábár *et al.*, 2012). Consequently, only large variations in the lattice parameter can be determined reliably from powder electron diffraction data and the typical accuracy of powder X-ray diffraction cannot be attained.

There are two main advantages of phase analysis from powders by electron diffraction compared with X-ray diffraction. First, much smaller volumes can be studied. Diffraction information can be collected from thin layers of a few tens of nanometres thickness, enabling precise identification of the inspected volume. If needed, different lateral sections from different depths of a bulk sample can be studied by TEM, thus providing three-dimensional information about the sample. In a non-homogeneous sample, electron diffraction data can be collected from different areas, allowing detection of different phases or texture components at a spatial resolution and sensitivity superior to X-ray diffraction methods (Lábár *et al.*, 2012).

The accuracy of the phase-content identification in a mixture for the major components is around 10–15% (Lábár *et al.*, 2012). The detection limit depends on the scattering power of the component. A weakly scattering phase of Cr in a strongly scattering matrix of Ag could only be detected at the content of 2%, while the presence of 5% Ag in a relatively weakly scattering Ni matrix allowed full quantification of the two phases (Lábár *et al.*, 2012). Thus, generally 5% (by volume) is accepted as the detection limit for powder electron diffraction experiments.

2.4.5. Texture analysis

By J. L. Lábár

The orientation distribution in a polycrystalline (nanocrystalline) TEM sample (used for powder electron diffraction) can either be random or a large fraction of grains can favour a special direction, *i.e.* the sample is textured. The texture can originate from the non-spherical shape of the particles (as in sedimentation geology or drop-drying of a suspension of nanoparticles on a TEM grid) or from energetic and/or kinetic conditions during nucleation and growth of grains in the formation of polycrystalline thin films on a substrate or, alternatively, the texture can be a result of mechanical deformation (as in drawing wires or rolling sheets of metals). Although the distribution of the preferred orientations can be very different, a few general types are frequently observed.

In the simplest case only one preferred-orientation vector characterizes the sample and the orientations of the grains are distributed arbitrarily around that direction. This situation is called *fibre texture* (single-axis texture). The most typical representatives of this texture class are sedimentation platy particles on a flat surface where the preferred-orientation vector is normal to the flat face of the particles, or a drawn metal wire where the preferred-orientation vector is directed along the wire axis. Another texture type frequently observed in the sedimentation of rod-shaped particles is described by the preferred-orientation vector being confined within a plane, but being arbitrarily oriented within this plane. Rolling of metal sheets results in other, more complex, but well characterized texture types: 'copper-type', 'brass-type' and 'S-type' (Mecking, 1985).

There are different ways to handle texture with electron diffraction. One approach is to collect the orientation information from individual nanograins in an automated area scan and reconstruct pole figures and inverse pole figures on a medium-sized population of grains (Rauch *et al.*, 2008). In principle, this is a single-crystal method analysing the information from an assembly of crystals. The Russian crystallography group developed the theory of arcs in oblique texture and used such textured patterns in structure analysis (Vainshtein, 1964; Vainshtein & Zvyagin, 1992). The *TexPat* software (Oleynikov & Hovmoller, 2004) was designed and effectively applied to determining unit-cell parameters and refining structure from oblique textured electron diffraction patterns. Tang *et al.* (1996) developed a method to determine the axis of texture and distribution of directions around that axis. The March–Dollase model (Dollase, 1986) for the description of pole densities was adapted for electron diffraction and used for the simulation of ring patterns (Li, 2010); however, no attempt was made to determine the phase fractions or textured fractions automatically.

A simplified automatic treatment of texture was implemented in the *ProcessDiffraction* software (Lábár, 2008, 2009). Partial texture is approximated by a linear combination of an ideally sharp fibre texture and a random distribution of components. Both the textured and the random components are treated as separately determined volume fractions during quantitative phase analysis (see Section 2.4.4). The advantage of the method is that the determination of the textured fraction is combined with simultaneous handling of a quasi-kinematic scattering by the Blackman approximation, and these two effects, which both modify the relative intensities, are treated simultaneously on a unified platform.

The application of the most general method for determining texture from powder electron diffraction patterns is restricted to the thinnest samples where kinematic scattering holds (Gemmi, Voltolini *et al.*, 2011). The method consists of recording a set of powder electron diffraction patterns at defined tilt steps of the two-axis goniometer, covering a considerable part of the solid-angle range usually used for recording pole figures. Azimuthal sections are integrated separately in 10° steps. The resulting large three-dimensional data set is fed into a variant of the Rietveld method called *MAUD* (Lutterotti *et al.*, 1997), which has built-in scattering factors for electrons. The orientation density function (ODF) is determined from the measured data by discretization of the orientation space. For texture fitting the *EWIMV* algorithm is used (Lutterotti *et al.*, 2004), which can be applied with irregular pole figure coverage and includes smoothing methods based on a concept of the tube projection. Pole figures from the smoothed

ODF were obtained for both sediment aggregates and evaporated thin films (Gemmi, Voltolini *et al.*, 2011).

2.4.6. Rietveld refinement with electron diffraction data

By T. E. Gorelik and U. Kolb

The Rietveld refinement method was initially developed for neutron diffraction data (Rietveld, 1967, 1969). It has now become a standard technique which is extensively used with neutron, laboratory X-ray and synchrotron diffraction data. A detailed description of the method can be found in Chapter 4.7.

Compared with the popularity of Rietveld refinement in X-ray and neutron powder diffraction, its application to powder electron diffraction data is very limited. So far, Rietveld refinement with electron diffraction data has only been done for nanocrystalline Al, α-MnS (Gemmi, Fischer *et al.*, 2011), hydroxyapatite (Song *et al.*, 2012), intermetallic AuFe (Luo *et al.*, 2011), TiO_2 (Weirich *et al.*, 2000; Tonejc *et al.*, 2002; Djerdj & Tonejc, 2005, 2006) and $MnFe_2O_4$ (Kim *et al.*, 2009). An example of a fit with powder electron diffraction data obtained by Rietveld refinement for hydroxyapatite is shown in Fig. 2.4.7.

Two major factors limit the application of Rietveld refinement to electron powder diffraction. First, electron powder diffraction data are collected from a sample volume far smaller than that used in an X-ray experiment. Therefore, the average statistics are poor compared with those of X-ray data. Nevertheless, electron powder diffraction data from a small sample area or thin films can give specific information which is difficult to obtain using other methods. Second, the presence of dynamical effects in the electron diffraction data hinders quantitative assessment of reflection intensities. Dynamical effects are strongest in zone-axis electron diffraction geometry, when many beams belonging to the same systematic rows are excited simultaneously. In powder electron diffraction crystals are randomly oriented towards the electron beam, thus making the fraction of zonal patterns low, thereby reducing the dynamical scattering in the data (see Section 2.4.2 for a more detailed discussion).

Within the limit of kinematical diffraction, the principle of Rietveld refinement is the same for electrons and X-rays, except the electron atomic scattering factors are different. The refinement procedure can thus be performed using existing programs if it is possible to input the scattering factors for electrons. Most of the reported Rietveld refinements on electron powder diffraction data have been performed using *FullProf* (Rodríguez-Carvajal, 1993); a refinement in *MAUD* (Lutterotti *et al.*, 1999) has also been reported (Gemmi, Voltolini *et al.*, 2011).

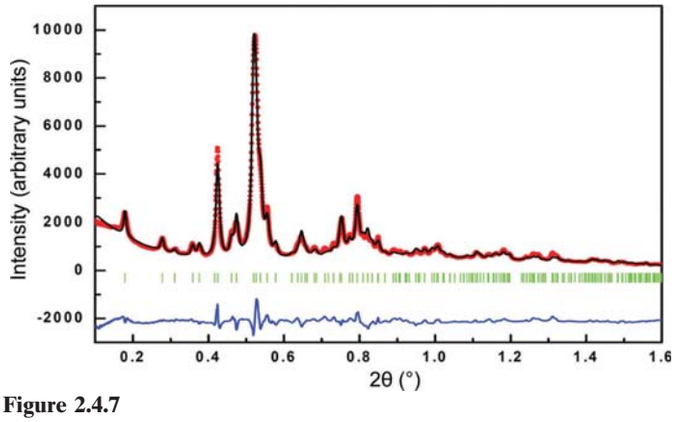

Figure 2.4.7
Rietveld analysis result with powder electron diffraction data of hydroxyapatite. Reproduced from Song *et al.* (2012) with permission from Oxford University Press.

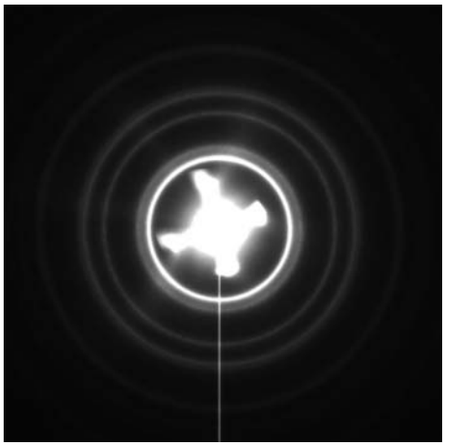

Figure 2.4.8
Powder electron diffraction pattern of nanocrystalline gold demonstrating non-symmetrical background features.

Electron powder diffraction patterns are recorded on an area detector. For a Rietveld refinement the two-dimensional diffraction patterns have to be integrated into one-dimensional profiles. The zero shift is treated as for the X-ray data integrated from a two-dimensional position-sensitive detector. Details about electron diffraction data processing and calibration are given in Section 2.4.3.4.

The background in electron powder patterns is a complex combination of inelastic scattering, scattering from the supporting film (when it is present) and other factors. For the Rietveld refinement procedure the background of a one-dimensional integrated profile is fitted by a polynomial function. If a supporting thin amorphous carbon film is used, the background can include broad rings, which after the one-dimensional integration can produce pronounced broad peaks. These peaks are difficult to subtract using a model based on a polynomial function; therefore, these intensities may hamper the powder diffraction profile matching (Kim *et al.*, 2009). In some cases, the background can even include radially non-symmetric features originating from the shape of the tip within the electron source (see Fig. 2.4.8); it can have blooming due to oversaturated CCD pixels, or streak shadows due to the fast transmission electron microscope beam-shutter movement. In these cases, a diffraction pattern from the adjacent 'empty' area of the sample can be acquired and subtracted from the diffraction pattern of the material prior to the integration into one dimension. This procedure allows elimination of some of the artifacts discussed above, which otherwise after the one-dimensional integration may be falsely interpreted as diffraction peaks, and are generally more difficult to fit.

Unit-cell parameters are mostly subject to the error due to the accuracy of the electron diffraction camera-length calibration. Although examples have been published showing 0.3% accuracy of the camera-length calibration, in most cases accuracy of about 2% can be achieved (Williams & Carter, 2009). The effective camera length depends on many instrumental parameters such as the convergence of the electron beam, the diffraction lens focus, the mechanical position of the sample within the objective lens, or the hysteresis of the electromagnetic lenses. Thus, while the ratio of the lattice parameters within one aligned diffraction pattern can be very precise, the absolute values might not be.

references